

## Exact scheme independence at two loops

Stefano Arnone\*

*Department of Physics and Astronomy,  
University of Southampton  
Highfield, Southampton SO17 1BJ, U.K.  
and Dipartimento di Fisica  
Università di Roma “La Sapienza”  
P.le Aldo Moro, 2 - 00185 Roma - Italy*

Antonio Gatti†

*DAMTP, Centre for Mathematical Sciences,  
Wilberforce Road, Cambridge CB3 0WA, U.K.*

Tim R. Morris‡ and Oliver J. Rosten§

*Department of Physics and Astronomy,  
University of Southampton  
Highfield, Southampton SO17 1BJ, U.K.  
(Dated: June 21, 2018)*

We further develop an algorithmic and diagrammatic computational framework for very general exact renormalization groups, where the embedded regularisation scheme, parametrised by a general cutoff function and infinitely many higher point vertices, is left unspecified. Calculations proceed iteratively, by integrating by parts with respect to the effective cutoff, thus introducing effective propagators, and differentials of vertices that can be expanded using the flow equations; many cancellations occur on using the fact that the effective propagator is the inverse of the classical Wilsonian two-point vertex. We demonstrate the power of these methods by computing the beta function up to two loops in massless four dimensional scalar field theory, obtaining the expected universal coefficients, independent of the details of the regularisation scheme.

PACS numbers: 11.10.Hi, 11.10.Gh

## I. INTRODUCTION AND CONCLUSIONS

The deeper understanding of renormalization, due to Wilson, follows most directly in the continuum from the exact renormalization group (ERG) flow equations [1]. The fact that solutions of these equations, for the Wilsonian effective action  $S$ , can be found directly in terms of renormalised quantities, that all physics (*e.g.* Green functions) can be extracted from  $S$ , and that renormalizability is trivially preserved in almost any approximation [2, 3], turns these ideas into a powerful framework for considering both perturbative and non-perturbative approximations (see for example refs. [1, 2, 3, 4, 5, 6, 7, 8, 9, 10, 11, 12, 13, 14, 15, 16, 17, 18, 19, 20, 21, 22, 23, 24, 25, 26]).

In the past a number of different versions and ways of deriving the ERG have been proposed [1, 2, 3, 4, 5, 6, 7, 9, 10, 21], which however have been shown to be equivalent under changes of variables [2, 3, 11, 12, 13]. Recently, far more general versions of the ERG have been considered

[13]. All the ERGs, including these generalised ones, can be seen to be parametrised by a functional  $\Psi$  [10, 13], that induces a reparametrisation (field redefinition) along the flow, and acts as a connection between the theory space of actions at different effective cutoff scales  $\Lambda$ . As a result, local to some generic point  $\Lambda$  on the flow, all these ERGs may be shown to be just reparametrisations of each other. When this reparametrisation can be extended globally, the result is an immediate proof of scheme independence for physical observables. Indeed computations of physical quantities then differ only through some field reparametrisation.

One practical example is an explicit field redefinition that interpolates between results computed using different choices of cutoff function [13]. Even more dramatic than this however, is the use of this freedom to adapt the ERG to certain forms of approximation or special physical problems [13]. In particular, recently there has been substantial progress in adapting these ideas to gauge theory. It turns out that not only can one introduce an effective cutoff  $\Lambda$  in a way that does not break the gauge invariance [28] but careful choices of  $\Psi$  allow the gauge invariance to be preserved manifestly, in fact not even gauge fixed, along the flow and in the solutions  $S$  [10, 14, 15].

Ref. [13] did not answer the question of precisely when the automatic local equivalence of two ERGs can be extended globally. In ref. [16], we showed that for four

\*Electronic address: stefano.arnone@roma1.infn.it

†Electronic address: A.Gatti@damtp.cam.ac.uk

‡Electronic address: T.R.Morris@soton.ac.uk; Currently at CERN, Theory Division, CH-1211 Genève 23, Switzerland

§Electronic address: O.J.Rosten@soton.ac.uk

dimensional one-component scalar field theory, the universal one-loop  $\beta$  function is obtained for a general form of  $\Psi$ , involving a very general ‘seed’ action  $\hat{S}$ . For simplicity we chose to keep  $\varphi \leftrightarrow -\varphi$  invariance ( $\varphi$  being the scalar field) and the  $\hat{S}$  two-point vertex was specified to be equal to that of the classical effective action, which thus determines them, up to a choice of cutoff function  $c$ . The only further requirements we imposed were that *the vertices of  $\hat{S}$  be infinitely differentiable and lead to convergent momentum integrals*. These easily met requirements are needed in any case for the ERG equation to make sense at the quantum level [16].

In this paper we will show that the universal two-loop  $\beta$  function also comes out correct for this very general form of  $\Psi$ . It is natural to conjecture then, that to all orders in perturbation theory, the only constraints required on  $\hat{S}$  to get universal answers for physical quantities are the ones in italics above. Furthermore, it is surely possible to show in perturbation theory, that all such ERGs are reparametrisations of each other, and indeed to construct the map perturbatively.

We will see that the iterative diagrammatic computational framework introduced in ref. [16], and further refined in the gauge theory context in ref. [15], extends straightforwardly to higher loops. The method works by turning the large redundancy in  $\Psi$  (here encapsulated in  $\hat{S}$ ) to our advantage. Since we are not allowed to inquire into the form of its vertices, the calculational steps are severely limited. The inherent generality thus acts as a roadmap to the most efficient computation. Indeed, since the form of the vertices is never specified, the majority of the calculation is best performed by manipulating the diagrams themselves.

However, it should be emphasised that, although the calculational procedure is the most efficient, the actual computation of the two-loop  $\beta$ -function, presented here, could be considerably shorter. Indeed, if our purpose were just to compute the two-loop  $\beta$ -function then, having used the redundancy of  $\Psi$  to uncover the best calculational procedure, we could use the simplest form of  $\hat{S}$  sufficient to yield a valid ERG. This corresponds to discarding all seed action vertices, other than the classical two-point vertex, reducing the ERG equation to Polchinski’s version. We would then be left with a powerful algorithmic and diagrammatic procedure, which does not require the cutoff function  $c$  to be specified.

Our aim is rather to explicitly demonstrate scheme independence and so we do not restrict  $\hat{S}$  in this way. Indeed, we even allow  $\hat{S}$  to have its own completely unspecified (loop) expansion in  $\hbar$ . Furthermore, by retaining a generic seed action, we gain valuable experience for the gauge theory case, where  $\hat{S}$  necessarily contains many interaction vertices [15].

An important prerequisite for this method to work, is that the effective action is written in self-similar form [27], in which no other explicit scale is introduced except  $\Lambda$ . (Note that although we formulate the method for a massless theory, nothing precludes the method from be-

ing applied to massive theories. The required self similar flow is achieved in this case simply by introducing the appropriate RG concept of a running mass, *i.e.* a function of  $\Lambda$  with its own  $\beta$  function, see for example [3, 17].)

We also constrain the form of the flow equation so that in this context, the kernel appearing in the ERG equation, is the differential of the effective propagator, the latter being the inverse of the classical effective action two-point vertex. (In gauge theory this condition holds only up to gauge transformations [15, 18].)

The computation then proceeds as follows. We introduce effective propagators in diagrams containing no explicit seed action vertices, by integrating by parts with respect to  $\Lambda$ . This results in total  $\Lambda$ -derivative contributions, and terms where the  $\Lambda$ -derivative acts on effective action vertices. We use the flow equation to process these latter further. Then, using the fact that the effective propagator is the inverse of the classical two-point vertex, many cancellations typically occur. The above procedure is repeated until there is no explicit dependence left upon the (generic) seed action  $\hat{S}$ . The whole of this iterative procedure may be performed entirely diagrammatically.

Universal terms arise from the total  $\Lambda$ -derivative contributions. Whenever the total  $\Lambda$ -derivative acts on convergent momentum integrals, the result follows trivially by dimensions; in particular, we frequently exploit the fact that dimensionless cases simply vanish. Although ultraviolet finiteness is built in to the ERG, non-vanishing universal terms arise from dimensionless momentum integrals that are infrared convergent only *after* the  $\Lambda$ -derivative is taken. At the two-loop level, we generate for the first time, contributions that are infrared divergent even after differentiation with respect to  $\Lambda$ . Of course at finite  $\Lambda$ , everything is infrared finite in the ERG, again by construction. Thus the game here is to rearrange so these infrared divergences cancel amongst each other; intelligent combinations of these terms then are convergent and vanish, or at worst result in calculable universal contributions.

In this way, the standard two-loop  $\beta$  function coefficient,  $-17/3(4\pi)^4$ , is derived, however without specifying at any stage the form of the cutoff function or the form of any of the higher point vertices.

We note that this two-loop  $\beta$  function coefficient has already been derived within the ERG, with various cutoff functions, and in various ways, corresponding to differing motivations [19, 20, 21, 22, 23, 24]. Although ref. [21] considered a general cutoff function, this work is the first to treat the more general case of an arbitrary seed action  $\hat{S}$  (corresponding to a continuum version of an arbitrary ‘blocking scheme’ [1]), and to reduce the computation in this general framework to a largely algorithmic and diagrammatic approach. We expect these insights to be especially useful for higher loop computations in the gauge invariant ERGs [25].

## II. A GENERALISED EXACT RENORMALIZATION GROUP EQUATION

We will consider a massless one-component scalar field theory in four Euclidean dimensions, and sketch the derivation of a generalised ERG equation, starting from Polchinski's equation [7]. For details we refer the reader to [16].

The Wilsonian renormalization group (RG) is defined in terms of some effective ultraviolet cutoff  $\Lambda$  [1]. Polchinski's version of Wilson's ERG equation [1] implements this transparently through a cutoff function  $c(p^2/\Lambda^2)$ , which modifies propagators  $1/p^2$  to  $\Delta = c/p^2$ . We take  $c$  to be *smooth*, *i.e.* infinitely differentiable, and always positive. It satisfies  $c(0) = 1$  so that low energies are unaltered, and tends to zero as  $p^2/\Lambda^2 \rightarrow \infty$  sufficiently fast that all Feynman diagrams are ultra-violet regulated.

The partition function is given as the functional integral of the measure,  $e^{-S}$ , where  $S$  is the Wilsonian effective action

$$S[\varphi; \Lambda] = \frac{1}{2} \int \frac{d^4 p}{(2\pi)^4} p^2 c_p^{-1} \varphi^2 + S^{int}[\varphi; \Lambda], \quad (1)$$

$c_p^{-1} \equiv c^{-1}(p^2/\Lambda^2)$ . The first term in the above, namely the regularised kinetic term, will be referred to as the seed action and denoted by  $\hat{S}$ .

Demanding that physics be invariant under the renormalization group transformation  $\Lambda \mapsto \Lambda - \delta\Lambda$ , results in a functional differential equation for the effective interaction [7], which can be recast in terms of the total effective action,  $S = \hat{S} + S^{int}$  [cf. eq. (1)],  $\Sigma \doteq S - 2\hat{S}$ , and the differentiated effective propagator  $\hat{\Delta} \doteq -\Lambda \partial_\Lambda \Delta = \frac{2}{\Lambda^2} c'(p^2/\Lambda^2)$ , as

$$\dot{S} \equiv -\Lambda \partial_\Lambda S = \frac{1}{2} \frac{\delta S}{\delta \varphi} \cdot \hat{\Delta} \cdot \frac{\delta \Sigma}{\delta \varphi} - \frac{1}{2} \frac{\delta}{\delta \varphi} \cdot \hat{\Delta} \cdot \frac{\delta \Sigma}{\delta \varphi} \quad (2)$$

(up to a vacuum energy term discarded in [7]. We will also refer to  $\hat{\Delta}$  as the kernel.)

In the above, prime denotes differentiation with respect to the function's argument (here  $p^2/\Lambda^2$ ) and the following shorthand has been introduced: for any two functions  $f(x)$  and  $g(y)$  and a momentum space kernel  $W(p^2/\Lambda^2)$ , with  $\Lambda$  being the effective cutoff,

$$f \cdot W \cdot g = \iint d^4 x d^4 y f(x) W_{xy} g(y), \quad (3)$$

where  $W_{xy} = \int \frac{d^4 p}{(2\pi)^4} W(p^2/\Lambda^2) e^{ip \cdot (x-y)}$ . ( $\hat{S}$  may therefore be written as  $\frac{1}{2} \partial_\mu \varphi \cdot c^{-1} \cdot \partial_\mu \varphi$ .)

Eq. (2), which is given diagrammatically as in fig. 1, can be turned into a flow equation for the measure,

$$\Lambda \partial_\Lambda e^{-S} = -\frac{1}{2} \frac{\delta}{\delta \varphi} \cdot \hat{\Delta} \cdot \left( \frac{\delta \Sigma}{\delta \varphi} e^{-S} \right), \quad (4)$$

which makes the invariance of the partition function under the renormalization group transformation manifest

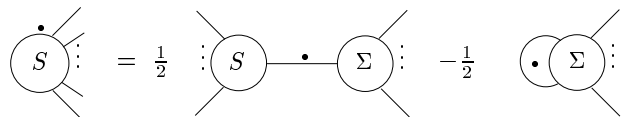


FIG. 1: Graphical representation of the ERG equation.  $S, \Sigma$   $n$ -point vertices are represented by circles labelled respectively by  $S, \Sigma$  with  $n$  legs attached, while bulleted lines stand for  $\hat{\Delta}$ .

by showing that the measure flows into a total functional derivative.

Eqs. (2), (4) may also be reinterpreted in a slightly different way: introducing  $\Psi = -\frac{1}{2\Lambda} \hat{\Delta} \frac{\delta \Sigma}{\delta \varphi}$  [13], we can regard the change in the partition function as corresponding to the field redefinition  $\varphi \rightarrow \varphi + \delta\Lambda \Psi$ , from which we can infer that integrating out degrees of freedom is just equivalent to a reparametrisation of the partition function [13, 14]. This somewhat counterintuitive result is allowed in the continuum because of the infinite number of degrees of freedom per unit volume.

Different forms of ERG equations are obtained by choosing different  $\Psi$ , and there is a great deal of freedom in such a choice of “blocking scheme” [13]. Nonetheless, physical quantities should not depend on the particular scheme, in other words they should turn out to be universal. Therefore we can choose a  $\Psi$  which is best suited for our purposes (for example one that generates a manifestly gauge invariant ERG [14, 15]) and still get the right answer when computing physical quantities.

Moreover, if physical results are to come out the same, irrespective of the choice of  $\Psi$ , we might well decide not to pick a specific form for it, but rather leave it general (except for some very general requirements discussed later) and implement a method for calculating universal quantities which does not depend on the details put in by hand. The main advantage of such a procedure is that we must be able to see that all the dependence of our results on unspecified quantities clearly cancels out.

In this paper we want to go along these lines and generalise our previous results [16] by calculating the two-loop beta function in a scalar field theory with a generalised  $\Psi$ . With so much freedom we have to restrict it to be able to be concrete; we choose to consider a general seed action  $\hat{S}$  of the form outlined below.

Firstly, we want the tree-level two-point vertex in  $\hat{S}$  to be the same as the required two-point vertex for the classical effective action. Since we are dealing with a massless theory, that means that both two-point vertices should be set to be equal to the regularised kinetic term in eq. (1)[29]. We will see in the next section that this constraint can be consistently imposed on solutions of the flow equation (2).

(In general we impose that the two-point vertices of  $\hat{S}$  and the effective action must coincide at the classical level. The form of the flow equations then imply that  $\hat{\Delta}$  really is the differentiated propagator in this context, *i.e.* the differential of  $\Delta$ , where  $\Delta$  is the inverse of the clas-

sical effective action two-point vertex. Here we already solved this constraint in writing eq. (2). However, for a massive theory, any classical mass would have to appear already in  $\Delta$ , thus slightly generalising eq. (2). Furthermore, in manifestly gauge invariant ERGs [14, 15], the inverse of the classical two-point vertex does not exist for the gauge fields; instead,  $\Delta$  is the inverse, only up to a gauge transformation. It is not necessary that the two-point vertices of  $\hat{S}$  and the classical effective action coincide. We choose to require this purely for the significant technical advantages it brings to our method, as described later.)

Secondly, we choose to leave the  $\varphi \leftrightarrow -\varphi$  symmetry alone, which implies that  $\hat{S}$  must be even under this symmetry. We are left with a generalised exact renormalization group parametrised by the infinite set of seed action  $2n$ -point vertices,  $n \geq 2$ . We will leave each of these vertices as completely unspecified functions of their momenta except for the very general requirements that *the vertices be infinitely differentiable and lead to convergent momentum integrals*. The first condition ensures that no spurious infrared singularities are introduced and that all effective vertices can be Taylor expanded in their momenta to any order [3, 10]. The second condition is necessary for the flow equation to make sense at the quantum level and also ensures that the flow actually corresponds to integrating out modes [13, 14].

We are therefore incorporating in the momentum dependence of *each* of the seed action  $2n$ -point vertices an infinite number of parameters. Of course these infinite number of vertices, each with an infinite number of parameters, then appear in the effective action  $S$  as a consequence of the flow equation. Remarkably, we can still compute the two-loop  $\beta$  function.

### III. PRELIMINARIES

#### A. Self-similar flow

We denote the vertices of the effective action as

$$S^{(2n)}(\vec{p}; \Lambda) \equiv S^{(2n)}(p_1, p_2, \dots, p_{2n}; \Lambda), \quad (5)$$

where we have factored out the momentum conserving  $\delta$  function:

$$(2\pi)^4 \delta\left(\sum_{i=1}^{2n} p_i\right) S^{(2n)}(\vec{p}; \Lambda) \doteq (2\pi)^{8n-4} \frac{\delta^{2n} S}{\delta\varphi(p_1) \cdots \delta\varphi(p_{2n})} \quad (6)$$

(and similarly for  $\hat{S}$ ).

In a standard perturbative treatment, we would define the theory, by stating that at the classical level the Lagrangian density takes the form

$$\frac{1}{2}(\partial_\mu\varphi)^2 + \frac{\lambda}{4!}\varphi^4. \quad (7)$$

After regularising the theory, the coupling is replaced by a bare coupling, and a bare mass is introduced, and these

are solved for, order by order in  $\lambda$ , so that at physical scales all quantities of physical interest (*e.g.* Green functions) are finite and correspond to a massless theory. An essential step in this treatment is to define what we really mean by  $\lambda$  through some renormalization condition.

If we regularise the theory, by using the cutoff function  $c$  at some ultra-violet cutoff scale  $\Lambda = \Lambda_0$ , then the Wilsonian effective action at physical scales  $S[\varphi; \Lambda]$  will simply result from integrating eq. (2), with the initial condition that  $S[\varphi; \Lambda_0]$  is the bare action. This can be done order by order in  $\lambda$ . In the continuum limit  $\Lambda_0 \rightarrow \infty$ , we obtain the Wilsonian effective action expressed in renormalized terms.

We will not approach the calculation this way. Instead, firstly we choose renormalization conditions that only involve the scale  $\Lambda$ , for example in this case we use

$$S^{(2)}(p; \Lambda) \equiv S^{(2)}(p, -p; \Lambda) = \sigma(\lambda)\Lambda^2 + p^2 + O(p^4/\Lambda^2), \quad (8)$$

$$S^{(4)}(\vec{0}; \Lambda) = \lambda, \quad (9)$$

where  $\sigma = \sigma_1\lambda + \sigma_2\lambda^2 + \dots$  is a function of  $\lambda$  which we determine self-consistently. This sets the physical mass to zero implicitly by ensuring that the only scale that appears is  $\Lambda$ , which itself tends to zero as all momenta are integrated out [30]. In order to obtain unit  $p^2$  coefficient in eq. (8), of course we also have to reparametrise the field by the wavefunction renormalization factor. In the limit that  $\Lambda_0 \rightarrow \infty$ , apart from the  $\Lambda$  dependence expected by naïve (*a.k.a.* engineering) dimensions, the only dependence on  $\Lambda$  then appears through  $\lambda(\Lambda)$ . Equivalently, if we rescale the field and positions/momenta by the appropriate (engineering) powers of  $\Lambda$  to make everything dimensionless, then the effective action takes the self-similar [27] form  $S[\varphi; \lambda]$ , in which *the only dependence on  $\Lambda$  is through the coupling  $\lambda(\Lambda)$* . The existence of such a solution is equivalent to a statement of renormalizability, and the solution corresponds to the renormalized trajectory [31] [3].

Secondly, we considerably simplify the analysis, both conceptually and in terms of procedure, by solving the ERG directly in terms of the self-similar solution  $S[\varphi; \lambda]$ , order by order in  $\lambda$  [2, 3, 10, 14, 15, 16, 17, 19]. In this way, we never introduce an overall cutoff (*e.g.*  $\Lambda_0$ ) or the notion of a bare action at all. Instead, we obtain the continuum physics directly.

#### B. Perturbative expansion

Rather than directly use the form of the flow equation in eq. (2), we first make explicit the wavefunction renormalization contribution. Moreover, we rescale  $\varphi$  so as to put the coupling constant in front of the action. This will ensure the expansion in the coupling constant coincides with the one in  $\hbar$ , the actual expansion parameter being

in fact  $\lambda\hbar$ . Our flow equation then reads [16]

$$\begin{aligned} & -\Lambda\partial_\Lambda \left( \frac{1}{\lambda} \tilde{S} \right) + \frac{\tilde{\gamma}}{2\lambda} \int_p \tilde{\varphi}(p) \frac{\delta \tilde{S}}{\delta \tilde{\varphi}(p)} \\ & = \frac{1}{2\lambda} \frac{\delta(\tilde{S} - 2\tilde{\hat{S}})}{\delta \tilde{\varphi}} \cdot \dot{\Delta} \cdot \frac{\delta \tilde{S}}{\delta \tilde{\varphi}} - \frac{1}{2} \frac{\delta}{\delta \tilde{\varphi}} \cdot \dot{\Delta} \cdot \frac{\delta(\tilde{S} - 2\tilde{\hat{S}})}{\delta \tilde{\varphi}}, \end{aligned} \quad (10) \quad S^{(4)}(\vec{0}; \Lambda) = 1. \quad (12)$$

where  $\int_p \equiv \int \frac{d^4 p}{(2\pi)^4}$  and a tilde has been put over rescaled quantities—so for example  $\tilde{\varphi} \equiv \frac{1}{\sqrt{\lambda}}\varphi$  and  $\tilde{S} \equiv \frac{1}{\lambda}S$ —as well as over the anomalous dimension  $\gamma$  ( $\gamma = \Lambda\partial_\Lambda \log Z$ ,  $Z$  being the wavefunction renormalization) to signify it has absorbed the change to  $\Lambda\partial_\Lambda|_{\tilde{\varphi}}$ .

(Note that eq. (10) is actually not the result of rescaling the wavefunction renormalization out of eq. (2). We must in addition change the cutoff function  $c \mapsto cZ$  in the flow equation [10, 13, 16]. However, the important point is that it clearly still satisfies the requirements of an ERG equation: namely that the partition function is invariant under the flow and that the flow corresponds to integrating out degrees of freedom [13, 15]. Hence it is a valid and even more appropriate starting point when the wavefunction renormalization is to be taken into account. This is another example of the immense freedom in the choice of the ERG equation.)

In order to simplify the notation, the tildes will be removed from now on. In these new, rescaled variables, the renormalization conditions are set to

$$S^{(2)}(p; \Lambda) \equiv S^{(2)}(p, -p; \Lambda) = \sigma(\lambda)\Lambda^2 + p^2 + O(p^4/\Lambda^2), \quad (11)$$

Both conditions are already saturated at tree level. (To see this it is sufficient to note that, since the theory is massless, the only scale involved is  $\Lambda$ . Since the tree-level four-point vertex is dimensionless, it must be a constant at null momenta. Thus  $S_0^{(4)}(\vec{0}; \Lambda) = S_0^{(4)}(\vec{0}; \Lambda_0) = 1$ , where the lower index 0 signifies the coupling is intended at the tree level. Similar arguments apply to the tree-level two-point function.)

Expanding the action, the seed action, the beta function  $\beta(\Lambda) = \Lambda\partial_\Lambda \lambda$  and the anomalous dimension in powers of the coupling constant, and bearing in mind that the (inverse of the) coupling constant now appears in front of  $S$ :

$$\begin{aligned} S[\varphi; \lambda] &= S_0 + \lambda S_1 + \lambda^2 S_2 + \dots, \\ \hat{S}[\varphi; \lambda] &= \hat{S}_0 + \lambda \hat{S}_1 + \lambda^2 \hat{S}_2 + \dots, \\ \beta(\Lambda) &= \beta_1 \lambda^2 + \beta_2 \lambda^3 + \dots, \\ \gamma(\Lambda) &= \gamma_1 \lambda + \gamma_2 \lambda^2 + \dots \end{aligned}$$

yields the loopwise expansion of the flow equation

$$\dot{S}_0 = \frac{1}{2} \frac{\delta S_0}{\delta \varphi} \cdot \dot{\Delta} \cdot \frac{\delta \Sigma_0}{\delta \varphi}, \quad (13)$$

$$\dot{S}_1 + \beta_1 S_0 + \frac{\gamma_1}{2} \varphi \cdot \frac{\delta S_0}{\delta \varphi} = \frac{\delta S_1}{\delta \varphi} \cdot \dot{\Delta} \cdot \frac{\delta \Pi_0}{\delta \varphi} - \frac{\delta S_0}{\delta \varphi} \cdot \dot{\Delta} \cdot \frac{\delta \hat{S}_1}{\delta \varphi} - \frac{1}{2} \frac{\delta}{\delta \varphi} \cdot \dot{\Delta} \cdot \frac{\delta \Sigma_0}{\delta \varphi}, \quad (14)$$

$$\dot{S}_2 + \beta_2 S_0 + \frac{\gamma_1}{2} \varphi \cdot \frac{\delta S_1}{\delta \varphi} + \frac{\gamma_2}{2} \varphi \cdot \frac{\delta S_0}{\delta \varphi} = \frac{\delta S_2}{\delta \varphi} \cdot \dot{\Delta} \cdot \frac{\delta \Pi_0}{\delta \varphi} - \frac{\delta S_0}{\delta \varphi} \cdot \dot{\Delta} \cdot \frac{\delta \hat{S}_2}{\delta \varphi} + \frac{1}{2} \frac{\delta S_1}{\delta \varphi} \cdot \dot{\Delta} \cdot \frac{\delta \Sigma_1}{\delta \varphi} - \frac{1}{2} \frac{\delta}{\delta \varphi} \cdot \dot{\Delta} \cdot \frac{\delta \Sigma_1}{\delta \varphi} \quad (15)$$

*etc.* where again dots above quantities signify  $-\Lambda\partial_\Lambda$ ,  $\Sigma_n = S_n - 2\hat{S}_n$  and  $\Pi_n = S_n - \hat{S}_n$ .

$\beta$  and  $\gamma$ , at one- and two-loop order, may be extracted directly from eqs. (14),(15), as specialised to the two- and four-point effective couplings, once the renormalization conditions have been taken into account.

The procedure is very straightforward: as the renormalization conditions are already saturated at tree level, there must be no quantum corrections to the two-point effective coupling at order  $p^2$ , nor to the four-point at

null momenta, *i.e.*

$$S_n^{(2)}(p; \Lambda) \Big|_{p^2} = S_n^{(4)}(\vec{0}; \Lambda) = 0 \quad \forall n \geq 1, \quad (16)$$

where the notation  $f|_{p^2}$  signifies that the coefficient of  $p^2$  in the series expansion of  $f$  must be taken. Hence the ERG equations for these special parts of the quantum corrections greatly simplify, reducing to algebraic equations which can be solved for  $\beta, \gamma$  at any order of perturbation theory.

As explained in the previous section, our  $\hat{S}$  is not completely arbitrary. Apart from the very general require-

ments on the differentiability and integrability of its vertices mentioned earlier, for convenience we restrict  $\hat{S}$  to have only even-point vertices, and constrain its tree-level two-point vertex so that it is equal to that of the classical effective action:

$$\hat{S}_0^{(2)}(p) = S_0^{(2)}(p). \quad (17)$$

Although this constraint is not necessary, it greatly simplifies the flow equations for higher point vertices, as it implies, for example, that  $\Pi_0^{(2)} \equiv 0$ . Recall that we also wish to set

$$S_0^{(2)}(p) = p^2 c_p^{-1}. \quad (18)$$

However,  $S_0^{(2)}(p)$  is already determined, up to an integration constant, by the flow equation. Using eq. (17) and the two-point part of eq. (13), and rearranging, we have

$$\Lambda \partial_\Lambda \left( S_0^{(2)}(p) \right)^{-1} = \Lambda \partial_\Lambda \Delta_p, \quad (19)$$

which shows that eq. (18) is consistent with the flow equation. Indeed,

$$S_0^{(2)}(p) \Delta_p = 1, \quad (20)$$

a central relation in the calculation that follows.




FIG. 2: Diagrammatic representation of eq. (20).

Before going to the details of the two-loop calculation, to which the next section will be devoted, we will describe what our method consists of by rederiving the one-loop contribution to  $\beta$  [16]. Being a much simpler calculation, it constitutes the perfect ground for illustrating our strategy and, moreover, it will help the reader to get familiar with the diagrammatics.

In order to ease notation in the figures, in what follows the vertices of the effective action will be labelled by their loop order only, and those of  $\hat{S}$  by their loop order with a “hat” on top.

### C. One-loop beta function

Specialising eq. (14) to the two- and four-point effective couplings and imposing the renormalization conditions, eq. (16), yields

$$\begin{aligned} \beta_1 + 2\gamma_1 &= 4S_1^{(2)}(0) \dot{\Delta}_0 \Pi_0^{(4)}(\vec{0}) - 4S_0^{(4)}(\vec{0}) \dot{\Delta}_0 \hat{S}_1^{(2)}(0) \\ &\quad - \frac{1}{2} \int_q \dot{\Delta}_q \Sigma_0^{(6)}(\vec{0}, q, -q), \end{aligned} \quad (21)$$

$$\begin{aligned} \beta_1 + \gamma_1 &= -2S_0^{(2)}(p) \dot{\Delta}_p \hat{S}_1^{(2)}(p) \Big|_{p^2} \\ &\quad - \frac{1}{2} \int_q \dot{\Delta}_q \Sigma_0^{(4)}(p, -p, q, -q) \Big|_{p^2}, \end{aligned} \quad (22)$$

where  $\dot{\Delta}_0 = \frac{2}{\Lambda^2} c'(0)$ . Eqs. (21), (22) are represented diagrammatically as in figs. 3, 4.

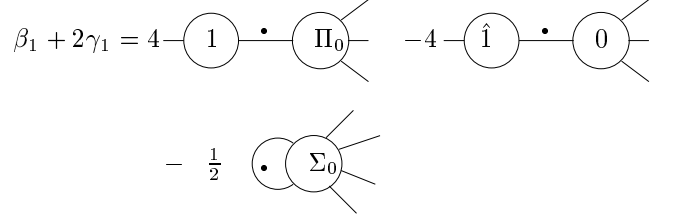


FIG. 3: Graphical representation of eq. (21). All the external legs have null momentum.

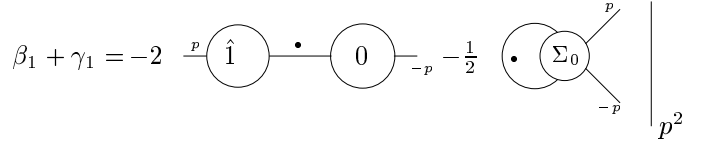


FIG. 4: Graphical representation of eq. (22).

We start processing eq. (22) by integrating by parts the diagram containing the four-point  $S_0$  vertex.

$$\begin{aligned} \beta_1 + \gamma_1 &= -\frac{1}{2} \int_q \left[ \Delta_q S_0^{(4)}(p, -p, q, -q) \right]_{p^2} \cdot + \frac{1}{2} \int_q \Delta_q \\ &\quad \times \dot{S}_0^{(4)}(p, -p, q, -q) \Big|_{p^2} + \int_q \dot{\Delta}_q \hat{S}_0^{(4)}(p, -p, q, -q) \Big|_{p^2} \\ &\quad - 2\hat{S}_1^{(2)}(p) \dot{\Delta}_p S_0^{(2)}(p) \Big|_{p^2}. \end{aligned} \quad (23)$$

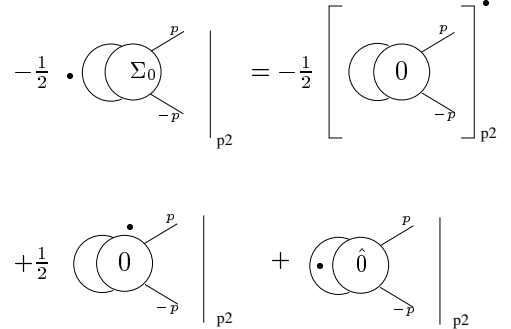


FIG. 5: Integrating by parts the four-point vertex in eq. (22) [cf. eq. (23)].

Now, the first term in the above represents a fully convergent integral [cf. eq. (23)], therefore the order of the derivative and integral signs can be exchanged. Moreover, as the integrand is dimensionless, there can be no dependence upon  $\Lambda$  after the momentum integral is carried out. Hence the result vanishes identically. The second term can be processed further by making use of the

tree-level flow equation for  $S_0^{(4)}(p, -p, q, -q)$ :

$$\frac{1}{2} \Delta_q \dot{S}_0^{(4)}(p, -p, q, -q) \Big|_{p^2} = \frac{1}{2} \Delta_q \left[ \hat{S}_0^{(4)}(p, -p, q, -q) \right. \\ \left. \times \left( -2S_0^{(2)}(p) \dot{\Delta}_p - 2S_0^{(2)}(q) \dot{\Delta}_q \right) \right]_{p^2} = -\dot{\Delta}_q$$

$$\times \hat{S}_0^{(4)}(p, -p, q, -q) \Big|_{p^2} - \Delta_q S_0^{(2)}(p) \dot{\Delta}_p \hat{S}_0^{(4)}(p, -p, q, -q) \Big|_{p^2}. \quad (24)$$

---

FIG. 6: Using the flow equation for  $S_0^{(4)}$ .

FIG. 7: Eq. (22) in its final form.

Using the relation  $S_0^{(2)}(q)\Delta_q = 1$  (*cf.* fig. 2), one of the two terms on the r.h.s. has been simplified. We can see that it just cancels the four-point  $\hat{S}$  contribution in eq. (23). The remaining one will cancel when eqs. (21), (22) are solved for  $\beta_1$ . Eq. (24) is shown in fig. 6, while

eq. (22) in its final form is displayed as in fig. 7.

We can diagrammatically process eq. (21) in pretty much the same way: integrating by parts and making use of the flow equation for the six-point effective coupling, we get the diagrams shown in fig. 8.

Having a closer look at fig. 8, we see that the terms containing six-point  $\hat{S}$  vertices cancel out (last diagram on the third row and first on the fourth). Moreover, the second and third diagrams on the fourth row pair up to give a  $\Pi$  four-point vertex, which in turn cancels against the first diagram on the third row. This is clear once this latter is expressed in terms of tree-level vertices. In more detail, the one-loop flow equation for the two-point coupling at null momentum is just given by fig. 5 except with  $p = 0$  and without the  $\mathcal{O}(p^2)$  restriction. With the same manipulations we get fig. 6, again without the order  $p^2$  restriction and with  $p = 0$  (causing the last term in fig. 6 to vanish). Thus we are only left with the total derivative in fig. 5, which can be integrated immediately to

$$S_1^{(2)}(0) = -\frac{1}{2} \int_q \Delta_q S_0^{(4)}(0, 0, q, -q), \quad (25)$$

with no integration constant since in a massless theory there must be no other explicit scale apart from the effective cutoff. The total derivative term in fig. 8 vanishes as there is no obstruction to exchanging the order of derivative and integral signs.

We still have to deal with the last three diagrams in fig. 8. Of these, we can only “attack” the one with no dependence upon  $\hat{S}$ , or else we would need to deal with the (generic) derivatives of the seed action vertices. So, integrating by parts and using the classical flow equations, the diagrams shown in fig. 10 are arrived at.

$$\begin{aligned}
\beta_1 + 2\gamma_1 &= 4 \text{---} \textcircled{1} \text{---} \textcircled{\Pi_0} \text{---} - 4 \text{---} \textcircled{\hat{1}} \text{---} \textcircled{0} \text{---} - \frac{1}{2} \text{---} \textcircled{\Sigma_0} \text{---} = \\
&= 4 \text{---} \textcircled{1} \text{---} \textcircled{\Pi_0} \text{---} - 4 \text{---} \textcircled{\hat{1}} \text{---} \textcircled{0} \text{---} - \frac{1}{2} \left[ \text{---} \textcircled{0} \text{---} \right]^\bullet + \frac{1}{2} \text{---} \textcircled{0} \text{---} + \text{---} \textcircled{\hat{0}} \text{---} = \\
&= 4 \text{---} \textcircled{1} \text{---} \textcircled{\Pi_0} \text{---} - 4 \text{---} \textcircled{\hat{1}} \text{---} \textcircled{0} \text{---} - \frac{1}{2} \left[ \text{---} \textcircled{0} \text{---} \right]^\bullet + \text{---} \textcircled{\hat{0}} \text{---} \\
&+ \frac{1}{2} \left[ -2 \text{---} \textcircled{\hat{0}} \text{---} + 4 \text{---} \textcircled{0} \text{---} \textcircled{0} \text{---} - 4 \text{---} \textcircled{0} \text{---} \textcircled{\hat{0}} \text{---} + \right. \\
&\quad \left. - 4 \text{---} \textcircled{\hat{0}} \text{---} \textcircled{0} \text{---} + 6 \text{---} \textcircled{0} \text{---} \textcircled{0} \text{---} - 12 \text{---} \textcircled{\hat{0}} \text{---} \textcircled{0} \text{---} \right]
\end{aligned}$$

FIG. 8: Using the flow equation for  $S_0^{(6)}$ . All the external lines carry zero momentum.

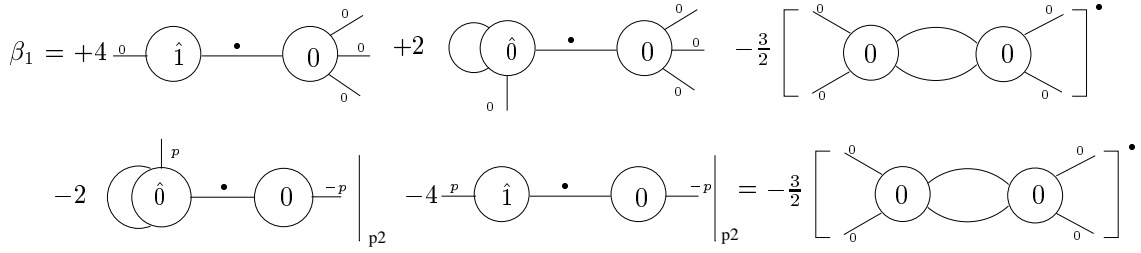
$$\text{---} \textcircled{1} \text{---} = -\frac{1}{2} \text{---} \textcircled{0} \text{---}$$

FIG. 9: Expressing  $S_1^{(2)}(0)$  in terms of tree-level vertices [cf. eq. (25)].

$$\begin{aligned}
\beta_1 + 2\gamma_1 &= -2 \text{---} \textcircled{\hat{0}} \text{---} \textcircled{0} \text{---} - 4 \text{---} \textcircled{\hat{1}} \text{---} \textcircled{0} \text{---} + 3 \text{---} \textcircled{0} \text{---} \textcircled{0} \text{---} \\
&- 6 \text{---} \textcircled{\hat{0}} \text{---} \textcircled{0} \text{---} = -2 \text{---} \textcircled{\hat{0}} \text{---} \textcircled{0} \text{---} - 4 \text{---} \textcircled{\hat{1}} \text{---} \textcircled{0} \text{---} \\
&+ \frac{3}{2} \left[ \text{---} \textcircled{0} \text{---} \textcircled{0} \text{---} \right]^\bullet - 3 \text{---} \textcircled{0} \text{---} \textcircled{0} \text{---} - 6 \text{---} \textcircled{\hat{0}} \text{---} \textcircled{0} \text{---} = \\
&- 4 \text{---} \textcircled{\hat{1}} \text{---} \textcircled{0} \text{---} - 2 \text{---} \textcircled{\hat{0}} \text{---} \textcircled{0} \text{---} + \frac{3}{2} \left[ \text{---} \textcircled{0} \text{---} \textcircled{0} \text{---} \right]^\bullet
\end{aligned}$$

FIG. 10: Further processing eq. (21), from fig. 8. All external legs carry zero momentum. To integrate by parts the second diagram, we use the fact that  $\Delta_q \hat{\Delta}_q = \frac{1}{2}(\Delta_q^2)^\bullet$ .



FIG. 11: Diagrammatic representation of  $\beta_1$ .

Collecting our results and solving for  $\beta_1$  we get just the five diagrams in fig. 11, of which only the third remains after the renormalization conditions are taken into account. In fact, as  $S_0^{(4)}(\vec{0}) = S_0^{(2)}(p)|_{p^2} = 1$ , the algebraic expressions corresponding to the other four diagrams cancel out in pairs.

In formulae,

$$\begin{aligned} \beta_1 &= \frac{3}{2} \int_q \frac{1}{q^4} \Lambda \partial_\Lambda \left\{ c_q S_0^{(4)}(0, 0, q, -q) \right\}^2 \\ &= -\frac{3}{2} \frac{\Omega_4}{(2\pi)^4} \int_0^\infty dq \partial_q \left\{ c_q S_0^{(4)}(0, 0, q, -q) \right\}^2 \\ &= \frac{3}{16\pi^2}, \end{aligned} \quad (26)$$

which is the standard one-loop result [32].

#### IV. TWO-LOOP BETA FUNCTION

This section is devoted to computing the two-loop beta function with a generalised seed action. The same procedure as in the previous section will be followed, namely:

- introduce integrated kernels in the diagrams containing effective action vertices only and integrate by parts so as to end up with a total  $\Lambda$ -derivative contribution plus terms where the  $\Lambda$ -derivative acts on the effective action vertices (*cf.* fig. 5);

- make use of the flow equation to process these latter further (*cf.* fig. 6);

- use the relation between the tree-level two-point vertex and the integrated kernel, eq. (20), *i.e.* fig. 2, to simplify the structure of the diagrams. At this point, many cancellations should become evident;

- repeat the above procedure when dealing with the diagrams generated by the use of the flow equations, until there is no dependence at all upon the (generic) seed action.

The one-loop relations, eqs. (21), (22), as well as eq. (25) will also be used to recast some terms in a more convenient form.

Moving on to the actual calculation, we start off by writing the RG equations for  $S_2^{(4)}(\vec{0})$  and  $S_2^{(2)}(p)|_{p^2}$ , which reduce to purely algebraic relations when the renormalization conditions are imposed. They take the form:

$$\begin{aligned} \beta_2 + 2\gamma_2 &= 4S_2^{(2)}(0) \dot{\Delta}_0 \Pi_0^{(4)}(\vec{0}) - 4\hat{S}_2^{(2)}(0) \dot{\Delta}_0 S_0^{(4)}(\vec{0}) \\ &\quad - 4S_1^{(2)}(0) \dot{\Delta}_0 \hat{S}_1^{(4)}(\vec{0}) - \frac{1}{2} \int_q \dot{\Delta}_q \Sigma_1^{(6)}(\vec{0}, q, -q), \end{aligned} \quad (27)$$

$$\begin{aligned} \beta_2 + \gamma_2 &= -2S_0^{(2)}(p) \dot{\Delta}_p \hat{S}_2^{(2)}(p)|_{p^2} + S_1^{(2)}(p) \dot{\Delta}_p \Sigma_1^{(2)}(p)|_{p^2} \\ &\quad - \frac{1}{2} \int_q \dot{\Delta}_q \Sigma_1^{(4)}(p, -p, q, -q)|_{p^2}, \end{aligned} \quad (28)$$

and are represented diagrammatically as in figs. 12, 13.

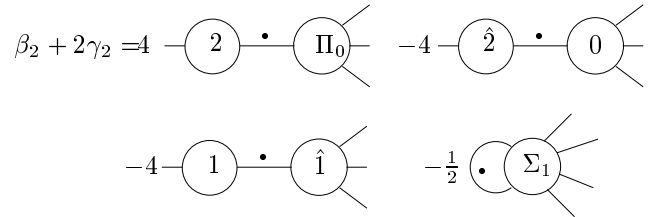


FIG. 12: Graphical representation of eq. (27). All the external legs have null momentum.

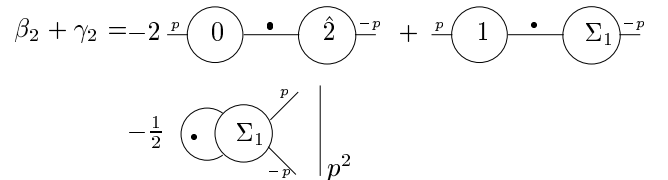


FIG. 13: Graphical representation of eq. (28).

It is easy to see that the algebraic expressions for the diagrams containing the seed action vertices at the highest possible loop order, *i.e.* the second in fig. 12 and the first in fig. 13, cancel out when solving for  $\beta_2$  once the

renormalization conditions, eq. (16), have been taken into account [*cf.* the comment below fig. 10]. Therefore, in what follows, those two diagrams will not appear in the graphical representations of eqs. (27), (28).

As in the one-loop case, we will start with the easier part, *i.e.* eq. (28). While the first two terms in fig. 13 need just expanding at order  $p^2$ , the third has to be fully processed.

Introducing the integrated kernel and making use of the flow equation for  $S_1^{(4)}(p, -p, q, -q)$  we get the contributions in fig. 14. Of these, we can only further simplify

v and vi, by unfolding the four- and six-point tree-level couplings together with the two-point one-loop vertex. The way forward is essentially the same as before, but with one *caveat*. Integrating by parts, that is trading  $\hat{\Delta}_q \sim 1/\Lambda^2$  for  $\Delta_q \sim 1/q^2$ , might cause the appearance of infrared divergences, absent in the first place as the ERG equation is well defined in the infrared. Of course, these divergences cancel out when all the diagrams on the r.h.s. are taken into account, but individual contributions might be infrared divergent. As an example, let us go back to fig. 14 and focus on v [33].

$$\begin{aligned}
 \beta_2 + \gamma_2 = & \text{ i. } \left[ \text{circle with } 1 \text{ and } p \text{ on top, } -p \text{ on bottom, and } \Sigma_1 \text{ on right} \right] - \frac{1}{2} \left[ \text{two overlapping circles with } 1 \text{ in the middle, } p \text{ on top, } -p \text{ on bottom} \right] - \frac{1}{2}(\beta_1 + 2\gamma_1) \left[ \text{two overlapping circles with } 0 \text{ in the middle, } p \text{ on top, } -p \text{ on bottom} \right] \\
 & + \text{ iv. } \left[ \text{two overlapping circles with } \Pi_0 \text{ in the middle, } p \text{ on top, } -p \text{ on bottom, and } 1 \text{ on right} \right] + \text{ v. } \left[ \text{two overlapping circles with } 1 \text{ on left, } \Pi_0 \text{ on right, } p \text{ on top, } -p \text{ on bottom} \right] - \frac{1}{4} \left[ \text{circle with } \Sigma_0 \text{ in the middle, } p \text{ on top, } -p \text{ on bottom, and a dot on top} \right] \\
 & - \text{ vii. } \left[ \text{two overlapping circles with } \hat{1} \text{ in the middle, } p \text{ on top, } -p \text{ on bottom, and } 0 \text{ on right} \right] - \text{ viii. } \left[ \text{two overlapping circles with } 0 \text{ on left, } \hat{1} \text{ on right, } p \text{ on top, } -p \text{ on bottom} \right] - \text{ ix. } \left[ \text{two overlapping circles with } \hat{1} \text{ on left, } 0 \text{ on right, } p \text{ on top, } -p \text{ on bottom, and a dot on top} \right] \Big|_{p^2}
 \end{aligned}$$

FIG. 14: Unfolding the one-loop four-point effective coupling.

Upon integration by parts we obtain the contributions shown in fig. 15.

Of these, the last two are clearly divergent. However their divergences must cancel out by construction, as the diagram on the l.h.s. of fig. 15 is infrared finite. In the case of the previous example, we could have written  $S_1^{(2)}(q) = [S_1^{(2)}(q)]_R + S_1^{(2)}(0)$ , which defines the reduced vertex,  $[S_1^{(2)}(q)]_R$ . The reduced vertex is at least  $\mathcal{O}(q^4)$ ,

and this is what we could have processed further. All the diagrams obtained by integration by parts would have been finite, containing either a reduced vertex or a  $\hat{\Delta}$ . For simplicity's sake, we will continue with the original method, bearing in mind that all infrared divergences indeed cancel out, which we will verify at the end of the calculation.

Returning to fig. 14 and iterating our procedure, we

obtain the diagrams in fig. 16.

Of those, i and iii vanish identically as they are

(ultraviolet- and) infrared-finite dimensionless integrals,

$$\begin{aligned}
& \text{Diagram with vertices } 1 \text{ and } \Pi_0 \text{ and a loop with a dot on } \Pi_0 \\
&= \text{Diagram with vertices } 1 \text{ and } 0 \text{ and a loop with a dot on } 0 \\
&\quad - \text{Diagram with vertices } 1 \text{ and } \hat{0} \text{ and a loop with a dot on } \hat{0} \\
&= \frac{1}{2} \left[ \text{Diagram with vertices } 1 \text{ and } 0 \text{ and a loop with a dot on } 0 \right] \\
&\quad + \frac{1}{2}(\beta_1 + \gamma_1) \text{Diagram with a dot on } 0 \\
&\quad + \text{Diagram with vertices } \hat{1} \text{ and } 0 \text{ and a loop with a dot on } \hat{1} \\
&+ \frac{1}{4} \text{Diagram with a dot on } \Sigma_0 \text{ and a loop with a dot on } 0 \\
&\quad + \text{Diagram with vertices } 1 \text{ and } \hat{0} \text{ and a loop with a dot on } \hat{0} \\
&\quad + \text{Diagram with vertices } 1 \text{ and } 0 \text{ and a loop with a dot on } 0
\end{aligned}$$

FIG. 15: Appearance of infrared divergences. External legs respectively carry  $p$  and  $-p$ .

$$\begin{aligned}
\beta_2 + \gamma_2 = & -\frac{1}{2} \left[ \text{Diagram i} \right] \cdot + \frac{1}{2} \left[ \text{Diagram ii} \right] \cdot - \frac{1}{8} \left[ \text{Diagram iii} \right] \cdot \\
& + \frac{1}{4} \left[ \text{Diagram iv} \right] \cdot + \frac{1}{6} \left[ \text{Diagram v} \right] \cdot + \frac{1}{2} \beta_1 \text{Diagram vi} \\
& + \text{Diagram vii} - \frac{1}{4} \text{Diagram viii} + \frac{1}{2} \text{Diagram ix} \\
& + \frac{1}{3} \text{Diagram x} - \text{Diagram xi}
\end{aligned}$$

FIG. 16: Eq. (28) in its final form. External legs carry momenta  $p$  and  $-p$  respectively. The r.h.s. must be evaluated at  $\mathcal{O}(p^2)$ .

so do ii and iv after their infrared-divergent parts have been cancelled against each other by means of fig. 9 [cf. eq. (25)]. (N.B. Neither ii nor iv is infrared divergent after the  $\Lambda$ -derivative is taken, however they each yield a finite non-zero answer. The strategy is that by combining the two diagrams we get one that is finite before differentiation, and thus zero afterwards.) We are then left with v, the wavefunction renormalization contribution to the beta function; vi, which will cancel a logarithmic divergence under a total  $\Lambda \partial_\Lambda$ , and with the last five diagrams, vii - xi, which all contain  $S_0^{(2)}(p)$ . Their corresponding algebraic expressions will cancel against similar contributions from eq. (27) by the renormalization conditions, in exactly the same fashion as described in fig. 11. Diagram

vi is arrived at by combining the expansion of i, iii, iv, viii in fig. 14 at order  $p^2$  together with that of other two diagrams coming from vi in the same figure and using fig. 7.

Let us now deal with eq. (27). In complete analogy with the one-loop calculation, we first solve the flow equation for the two-point coupling at null momentum. The two-loop analogue of eq. (25) is shown in fig. 17. (As before, the first two diagrams are actually infrared divergent, but the divergent parts cancel out if eq. (25) is taken into account.)

Next, we process the second diagram in fig. 12. After several iterations, we arrive at the final form for eq. (27), shown in fig. 18.

$$\begin{aligned}
\text{---} \circlearrowleft 2 \text{---} &= \frac{1}{2} \left[ \text{---} \circlearrowleft 1 \text{---} \circlearrowleft 0 \text{---} \right] + \frac{1}{4} \left[ \text{---} \circlearrowleft 0 \text{---} \circlearrowleft 0 \text{---} \right] + \frac{1}{6} \left[ \text{---} \circlearrowleft 0 \text{---} \circlearrowleft 0 \text{---} \right] \\
&\quad - \frac{1}{8} \left[ \text{---} \circlearrowleft 0 \text{---} \circlearrowleft 0 \text{---} \right] - \frac{1}{2} \left[ \text{---} \circlearrowleft 1 \text{---} \circlearrowleft 0 \text{---} \right]
\end{aligned}$$

FIG. 17: Diagrammatical solution of the flow equation for  $S_2^{(2)}(0)$ .

$$\begin{aligned}
\beta_2 + 2\gamma_2 = & -\frac{1}{2} \left[ \text{---} \circlearrowleft 1 \text{---} \right]^\bullet + \frac{1}{2} \left[ \text{---} \circlearrowleft 1 \text{---} \circlearrowleft 0 \text{---} \right]^\bullet + 3 \left[ \text{---} \circlearrowleft 1 \text{---} \circlearrowleft 0 \text{---} \right]^\bullet \\
& - \frac{1}{8} \left[ \text{---} \circlearrowleft 0 \text{---} \right]^\bullet + \frac{3}{2} \left[ \text{---} \circlearrowleft 0 \text{---} \circlearrowleft 0 \text{---} \right]^\bullet + \frac{2}{3} \left[ \text{---} \circlearrowleft 0 \text{---} \circlearrowleft 0 \text{---} \right]^\bullet \\
& - 3 \left[ \text{---} \circlearrowleft 0 \text{---} \circlearrowleft 0 \text{---} \right]^\bullet - \frac{3}{2} \left[ \text{---} \circlearrowleft 0 \text{---} \circlearrowleft 0 \text{---} \right]^\bullet - 3 \left[ \text{---} \circlearrowleft 0 \text{---} \circlearrowleft 0 \text{---} \right]^\bullet \\
& - \frac{3}{4} \left[ \text{---} \circlearrowleft 0 \text{---} \circlearrowleft 0 \text{---} \circlearrowleft 0 \text{---} \right]^\bullet + \beta_1 \left[ \text{---} \circlearrowleft 0 \text{---} \right]^\bullet - 3\beta_1 \left[ \text{---} \circlearrowleft 0 \text{---} \circlearrowleft 0 \text{---} \right]^\bullet \\
& + \frac{1}{4} \left[ \text{---} \circlearrowleft 0 \text{---} \circlearrowleft 0 \text{---} \right]^\bullet + 2 \left[ \text{---} \circlearrowleft 1 \text{---} \hat{0} \text{---} \bullet \text{---} \circlearrowleft 0 \text{---} \right]^\bullet - \frac{1}{2} \left[ \text{---} \circlearrowleft \hat{0} \text{---} \bullet \text{---} \circlearrowleft 0 \text{---} \right]^\bullet \\
& + \left[ \text{---} \circlearrowleft 0 \text{---} \circlearrowleft \hat{0} \text{---} \bullet \text{---} \circlearrowleft 0 \text{---} \right]^\bullet + \frac{2}{3} \left[ \text{---} \circlearrowleft 0 \text{---} \circlearrowleft \hat{0} \text{---} \bullet \text{---} \circlearrowleft 0 \text{---} \right]^\bullet - 2 \left[ \text{---} \circlearrowleft \hat{1} \text{---} \bullet \text{---} \circlearrowleft 0 \text{---} \right]^\bullet
\end{aligned}$$

FIG. 18: Eq. (27) in its final form. External legs carry zero momenta.

Again, there are many cancellations. In detail, i, iii, iv and vi vanish identically as they are convergent and di-

dimensionless [34], and so do ii and xiii after their infrared-divergent parts have been cancelled against each other.

Moreover, the infrared-divergent part of  $v$  results in the finite contribution  $-\beta_1 \int_k S_0^{(6)}(\vec{0}, k, -k) \Delta_k$ , which cancels xi exactly. In a somewhat similar fashion, we see that the divergent part [35] of viii is equal and opposite to that of vii, up to a term that will cancel vi in fig. 16, *i.e.*

$$(viii)_{\text{div}} = -(vii)_{\text{div}} + \beta_1 \int_k S_0^{(4)}(q, -q, k, -k) \Delta_k \Big|_{q^2}. \quad (29)$$

(In more detail, by the renormalization conditions  $S_1^{(2)}(q)$

has no  $\mathcal{O}(q^2)$  part, its zeroth order part being that of fig. 9. On the contrary, the  $\mathcal{O}(q^2)$  part in viii remains uncanceled.) Diagrams xi and xii again result from pairing up several topologically different diagrams and using fig. 7.

As for the last five diagrams, xiv - xviii, they respectively cancel the last five terms in fig. 16 when the two equations are solved for  $\beta_2$ . Hence, the only diagrams to be evaluated are those in fig. 19.

$$\beta_2 = +\frac{1}{3} \left[ \begin{array}{c} p \quad \text{---} \quad \text{---} \quad -p \\ \circ \quad \text{---} \quad \text{---} \quad \circ \\ \text{---} \quad \text{---} \quad \text{---} \end{array} \right] p^2 + 3 \left[ \begin{array}{c} \text{---} \quad \text{---} \quad \text{---} \\ \circ \quad \text{---} \quad \circ \\ \text{---} \quad \text{---} \quad \text{---} \\ \circ \quad \text{---} \quad \circ \\ \text{---} \quad \text{---} \end{array} \right] + \frac{3}{4} \left[ \begin{array}{c} \text{---} \quad \text{---} \quad \text{---} \\ \circ \quad \text{---} \quad \circ \quad \text{---} \quad \circ \\ \text{---} \quad \text{---} \quad \text{---} \end{array} \right] + 3\beta_1 \left[ \begin{array}{c} \text{---} \quad \text{---} \\ \circ \quad \text{---} \quad \circ \\ \text{---} \quad \text{---} \end{array} \right]$$

FIG. 19: Contributions to  $\beta_2$ .

The first three are already expressed as total derivatives, whereas the fourth can be turned into one by means

of eq. (26) (*cf.* fig. 20).

$$+3\beta_1 \left[ \begin{array}{c} \text{---} \quad \text{---} \\ \circ \quad \text{---} \quad \circ \\ \text{---} \quad \text{---} \end{array} \right] = 3 \left(-\frac{3}{2}\right) \left[ \begin{array}{c} \text{---} \quad \text{---} \\ \circ \quad \text{---} \quad \circ \\ \text{---} \quad \text{---} \end{array} \right] \cdot \left[ \begin{array}{c} \text{---} \quad \text{---} \\ \circ \quad \text{---} \quad \circ \\ \text{---} \quad \text{---} \end{array} \right] \\ = -\frac{9}{4} \left[ \begin{array}{c} \text{---} \quad \text{---} \quad \text{---} \\ \circ \quad \text{---} \quad \circ \quad \text{---} \quad \circ \\ \text{---} \quad \text{---} \end{array} \right] \cdot \left[ \begin{array}{c} \text{---} \quad \text{---} \quad \text{---} \\ \circ \quad \text{---} \quad \circ \quad \text{---} \quad \circ \\ \text{---} \quad \text{---} \end{array} \right]$$

FIG. 20: Turning last term in fig. 19 into a total derivative.

Although trading a numerical coefficient,  $\beta_1$ , for a diagram might be regarded as an added complication, it actually greatly simplifies the rest of the calculation, as we now just need to extract the infrared part of each diagram. In order to do this, the reduced four-point vertices are introduced, which by construction (and Lorentz invariance) vanish at least as the following powers of mo-

mentum:

$$S_R(k) \doteq S_0^{(4)}(0, 0, k, -k) - S_0^{(4)}(\vec{0}) = \mathcal{O}(k^2), \\ S_R(k, q) \doteq S_0^{(4)}(k, -k, q, -q) - S_0^{(4)}(k, -k, 0, 0) \\ - S_0^{(4)}(0, 0, q, -q) + S_0^{(4)}(\vec{0}) = \mathcal{O}(q \cdot k).$$

Eliminating all four-point vertices in favour of the reduced ones, we can easily single out the infrared-divergent parts, discarding finite contributions which

would vanish after the derivative with respect to  $\Lambda$  is taken.

The third term in fig. 19, for example, can be written as

$$\begin{aligned}
& \frac{3}{4} \int_{k,q} S_0^{(4)}(0,0,q,-q) \Delta_q^2 S_0^{(4)}(q,-q,k,-k) \\
& \times \Delta_k^2 S_0^{(4)}(0,0,k,-k) \\
& = \frac{3}{4} \int_{k,q} \left( S_R(q) + 1 \right) \Delta_q^2 \left( S_R(k,q) + S_R(k) \right. \\
& \left. + S_R(q) + 1 \right) \Delta_k^2 \left( S_R(k) + 1 \right) \\
& = \frac{3}{4} \int_{k,q} \left[ 2 \left( S_R(q) + 1 \right)^2 - 1 \right] \Delta_q^2 \Delta_k^2 \\
& = \frac{3}{4} \int_{k,q} \left[ 2S^2(q) - 1 \right] \Delta_q^2 \Delta_k^2,
\end{aligned}$$

where  $S(q)$  stands for (the un-reduced)  $S_0^{(4)}(0,0,q,-q)$ .

The diagram in fig. 20 has exactly the same structure, but with  $-\frac{9}{4}$  in front. The second term in fig. 19 can be simplified to

$$3 \int_{k,q} \left[ S(q)^2 \Delta_k^2 \Delta_q \Delta_{k+q} \right]^\bullet. \quad (30)$$

Putting the three together yields

$$\begin{aligned}
& 3 \int_{k,q} \left[ S(q)^2 \Delta_k^2 \Delta_q \left( \Delta_{k+q} - \Delta_q \right) \right]^\bullet + \frac{3}{2} \int_{k,q} \left[ \Delta_q^2 \Delta_k^2 \right]^\bullet \\
& = 3 \int_{k,q} \left[ \Delta_k^2 \Delta_q \left( \Delta_{k+q} - \Delta_q \right) \right]^\bullet + \frac{3}{2} \int_{k,q} \left[ \Delta_q^2 \Delta_k^2 \right]^\bullet \\
& = 3 \int_{k,q} \left[ \Delta_k^2 \Delta_q \left( \Delta_{k+q} - \frac{1}{2} \Delta_q \right) \right]^\bullet,
\end{aligned} \quad (31)$$

where we again used  $S(q) = S_R(q) + 1$  to discard the contributions that are infrared finite before differentiation with respect to  $\Lambda$ . As regards the first diagram in fig. 19, it amounts to

$$\begin{aligned}
& \frac{1}{3} \int_{k,q} \left[ \left( S_0^{(4)}(-p,k,q+p,-k-q) \right)^2 \Delta_k \Delta_{q+k} \Delta_{q+p} \right]_{p^2}^\bullet \\
& = \frac{1}{3} \int_{k,q} \left[ \left( S_0^{(4)}(0,k,q,-k-q) \right)^2 \Delta_k \Delta_{q+k} \Delta_{q+p} \right]_{p^2}^\bullet \\
& = \frac{1}{3} \int_{k,q} \left[ \Delta_k \Delta_{q+k} \Delta_{q+p} \right]_{p^2}^\bullet,
\end{aligned} \quad (32)$$

as the only non-vanishing contribution comes from taking the order  $p^2$  from one of the propagators.

The integrals (31),(32), representing the usual contributions to the two-loop beta function, can be easily computed for a generic cutoff function if Bonini's lead [21] is followed. It consists in "eliminating" one of the cutoff

functions by writing, say,  $c_q = (c_q - 1) + 1$  and neglecting the first term as it is already of order  $q^2$ . This, of course, can only be done if the integrand remains UV regulated afterwards and if the  $\mathcal{O}(q^2)$  part indeed makes the integral infrared convergent.

Taking eq. (32) as an example, we can trade  $c_k$  for 1, *e.g.*

$$\begin{aligned}
& \frac{1}{3} \int_{k,q} \left[ \Delta_k \Delta_{q+k} \Delta_{q+p} \right]_{p^2}^\bullet = \frac{1}{3} \int_{k,q} \left[ \frac{1}{k^2} \Delta_{q+k} \Delta_{q+p} \right]_{p^2}^\bullet \\
& = \frac{2}{3} \int_{k,q} \frac{1}{(k-q)^2} \Delta_k \left( \frac{2}{\Lambda^2} c'_{q+p} \right)_{p^2},
\end{aligned}$$

where the last equality follows from taking the derivative with respect to  $\Lambda$  and shifting  $k \rightarrow k - q$ .

Averaging over the angles and taking the order  $p^2$ , we arrive at the final result (the calculation is detailed in the appendix),

$$\frac{2}{3} \int_{k,q} \frac{1}{(k-q)^2} \Delta_k \left( \frac{2}{\Lambda^2} c'_{q+p} \right)_{p^2} = \frac{1}{3} \left( \frac{1}{16\pi^2} \right)^2. \quad (33)$$

The integral in eq. (31) can be dealt with in pretty much the same way (for the details see the appendix):

$$\begin{aligned}
& 3 \int_{k,q} \left[ \Delta_k^2 \Delta_q \left( \Delta_{k+q} - \frac{1}{2} \Delta_q \right) \right]^\bullet = 3 \int_{k,q} \frac{(c_k^2 c_q^2)^\bullet}{k^4 q^2} \\
& \times \left( \frac{1}{(k+q)^2} - \frac{1}{2q^2} \right) = -6 \left( \frac{1}{16\pi^2} \right)^2,
\end{aligned}$$

and summing up the two contributions the standard result follows:

$$\beta_2 = -\frac{17}{3} \left( \frac{1}{16\pi^2} \right)^2. \quad (34)$$

### Acknowledgments

We acknowledge financial support from PPARC Rolling grant PPA/G/O/2000/00464 (TRM, SA), PPARC SPG PPA/G/S/1998/00527 (AG) and the Southampton University Development Trust (OJR).

### APPENDIX A: THE EVALUATION OF TWO-LOOP INTEGRALS

This appendix is devoted to the detailed calculation of (31), (32).

Let us consider first the wavefunction renormalization contribution, eq. (32). Rewriting  $c_k$  as  $(c_k - 1) + 1$ , we see that  $(c_k - 1)$  already makes the integral convergent in the infrared, thus giving a vanishing contribution when the derivative with respect to  $\Lambda$  is taken. Therefore we only retain the 1:

$$\frac{1}{3} \int_{k,q} \left[ \Delta_k \Delta_{q+k} \Delta_{q+p} \right]_{p^2}^\bullet = \frac{1}{3} \int_{k,q} \left[ \frac{1}{k^2} \Delta_{q+k} \Delta_{q+p} \right]_{p^2}^\bullet. \quad (A1)$$

Taking the  $\Lambda$ -derivative and bearing in mind the permutation symmetry in the three momenta:

$$\frac{2}{3} \int_{k,q} \frac{1}{(k-q)^2} \Delta_k \left( \frac{2}{\Lambda^2} c'_{q+p} \right)_{p^2}, \quad (\text{A2})$$

where we have also shifted  $k$  to  $k-q$ . Defining  $\theta_k$  to be the angle between the Euclidean 4-vectors [36]  $k$  and  $q$ , *i.e.*  $k \cdot q \doteq kq \cos \theta_k$ , we can perform the angular integration in  $k$  to get

$$\begin{aligned} & \frac{4}{3\Lambda^2} \int_q c'_{q+p} \Big|_{p^2} \int_0^\infty dk k^3 \Delta_k \int \frac{d\Omega_k}{(2\pi)^4} \frac{1}{(k-q)^2} \\ &= \frac{4\mathcal{Q}_4}{3\Lambda^2} \int_q c'_{q+p} \Big|_{p^2} \int_0^\infty dk \frac{k c_k}{\max\{k^2, q^2\}}, \end{aligned}$$

where  $\mathcal{Q}_4$  is the four-dimensional solid angle divided by  $(2\pi)^4$ . Expanding  $c'_{q+p}$  to take the order  $p^2$  and defining  $\theta_q$  as the angle between  $q$  and  $p$ , we can integrate over the solid angle,  $d\Omega_q$ ,

$$\frac{4\mathcal{Q}_4}{3\Lambda^4} \int_0^\infty dq q^3 \left( c''_q + \frac{q^2}{2\Lambda^2} c'''_q \right) \left\{ \int_0^q dk \frac{k c_k}{q^2} + \int_q^\infty dk \frac{c_k}{k} \right\}. \quad (\text{A3})$$

We now introduce two dimensionless variables,  $x = \frac{k^2}{\Lambda^2}$ ,  $y = \frac{q^2}{\Lambda^2}$  and recast the above as

$$\frac{\mathcal{Q}_4}{3} \int_0^\infty dy \left( c''_y + \frac{y}{2} c'''_y \right) \left\{ \int_0^y dx c_x + \int_y^\infty dx y \frac{c_x}{x} \right\}, \quad (\text{A4})$$

with  $c_x^{(n)}$  being  $c^{(n)}(x)$  and similarly for  $y$ .

Exchanging the order of integration, so that the integral over  $y$  is performed first, and temporarily discarding the numerical factor in front of the integral

$$\begin{aligned} & \int_0^\infty dx c_x \left\{ \int_x^\infty dy \left( c''_y + \frac{y}{2} c'''_y \right) + \int_0^x dy \left( \frac{y}{x} c''_y + \frac{y^2}{2x} c'''_y \right) \right\} = \\ & \left\{ -\frac{1}{2} x c_x c'_x \Big|_0^\infty + \frac{1}{2} \int_0^\infty dx x (c'_x)^2 + \int_0^\infty dx \frac{c_x x^2}{x} c''_x \right\} = \\ & \left( -\frac{1}{4} c_x^2 \right)_0^\infty = \frac{1}{4}. \end{aligned}$$

- [1] K. G. Wilson, *Phys. Rev.* **D 10** (1974) 2445; F.J. Wegner and A. Houghton, *Phys. Rev.* **A 8** (1973) 401; K. G. Wilson in *New Phenomena in Subnuclear Physics* (Eric '75), ed. A. Zichichi (Plenum Press, New York, 1977); K. G. Wilson in *Recent Developments in Gauge Theories* (Cargèse '79), ed. G. 't Hooft (Plenum Press, New York, 1980).
- [2] Tim R. Morris, *Int. J. Mod. Phys.* **A 9** (1994) 2411, [hep-ph/9308265](#).
- [3] Tim R. Morris, in *Yukawa International Seminar '97*, *Prog. Theor. Phys. Suppl.* **131** (1998) 395, [hep-th/9802039](#).
- [4] A. Hasenfratz and P. Hasenfratz, *Nucl. Phys.* **B 270** (1986) 687.
- [5] T.R. Morris, in *New Developments in Quantum Field Theory*, NATO ASI series 366, (Plenum Press, 1998); J.

Hence, eq. (32) amounts to

$$\frac{1}{4} \frac{\mathcal{Q}_4^2}{3} = \frac{1}{3} \left( \frac{1}{16\pi^2} \right)^2. \quad (\text{A5})$$

As far as eq. (31) is concerned, we can follow the same strategy and write  $c_{k+q} = (c_{k+q} - c_q) + c_q$ , retaining only  $c_q$ :

$$\begin{aligned} & 3 \int_{k,q} \left[ \Delta_k^2 \Delta_q \left( \Delta_{k+q} - \frac{1}{2} \Delta_q \right) \right]^\bullet \\ &= 3 \int_{k,q} \frac{(c_k^2 c_q^2)^\bullet}{k^4 q^2} \left( \frac{1}{(k+q)^2} - \frac{1}{2q^2} \right). \end{aligned}$$

Averaging over the angles and rewriting in terms of  $x, y$  we get

$$\begin{aligned} & \frac{3}{2} \mathcal{Q}_4 \left\{ \int_0^\infty dx \int_0^x dy \left[ \frac{c_x^2}{x^2} y (c_y^2)' + \frac{(c_x^2)'}{x} c_y^2 \right] \right. \\ & \quad + \frac{1}{2} \int_0^\infty dx \int_x^\infty dy \left[ \frac{c_x^2}{x} (c_y^2)' + (c_x^2)' \frac{c_y^2}{y} \right] \\ & \quad \left. - \frac{1}{2} \int_0^\infty dx \int_0^x dy \left[ \frac{c_x^2}{x} (c_y^2)' + (c_x^2)' \frac{c_y^2}{y} \right] \right\}. \quad (\text{A6}) \end{aligned}$$

Again exchanging the order of integration and using the fact that the integrand is invariant under the exchange  $x \leftrightarrow y$ , we see the last two lines in eq. (A6) are equal and opposite, while the first can be rewritten as

$$\begin{aligned} & \frac{3}{2} \mathcal{Q}_4 \left[ \frac{c_x^2}{x} \int_0^x dy c_y^2 \right]_{x=0}^\infty = - \lim_{x \rightarrow 0} \frac{3}{2} \mathcal{Q}_4 \frac{c_x^2}{x} \int_0^x dy c_y^2 \\ &= -\frac{3}{2} \mathcal{Q}_4^2 = -6 \left( \frac{1}{16\pi^2} \right)^2. \end{aligned}$$

- Berger, N. Tetradis and C. Wetterich, [hep-ph/0005122](#); C. Bagnuls and C. Bervillier, *Phys. Rep.* **348** (2001) 91; J. Polonyi, [hep-th/0110026](#).
- [6] S. Weinberg, Erice lectures, *Subnucl. Phys.* (1976) 1; J. F. Nicoll and T. S. Chang, *Phys. Lett.* **A 62** (1977) 287.
- [7] J. Polchinski, *Nucl. Phys.* **B 231** (1984) 269. G. Gallavotti, *Rev. Mod. Phys.* **57** (1985) 471.
- [8] Bonini *et al.*, *Nucl. Phys.* **B 409** (1993) 441, [hep-th/9301114](#).
- [9] C. Wetterich, *Phys. Lett.* **B 301** (1993) 90.
- [10] Tim R. Morris, in *The Exact Renormalization Group*, eds Krasnitz *et al.*, World Scientific (1999) 1.
- [11] T. R. Morris, *Phys. Lett.* **B 329** (1994) 241, [hep-ph/9403340](#); *Phys. Lett.* **B 334** (1994) 355, [hep-th/9405190](#); *Nucl. Phys.* **B 458**[FS] (1996) 477, [hep-th/9508017](#).

- [12] J.-I. Sumi, W. Souma, K.-I. Aoki, H. Terao and K. Morikawa, [hep-th/0002231](#).
- [13] Jose I. Latorre and Tim R. Morris, *J. High Energy Phys.* **0011** (2000) 004.
- [14] Tim R. Morris, *Nucl. Phys.* **B 573** (2000) 97; *J. High Energy Phys.* **0012** (2000) 12.
- [15] S. Arnone, A. Gatti and T.R. Morris, *Phys. Rev.* **D67** (2003) 085003.
- [16] S. Arnone, A. Gatti and T.R. Morris, *J. High Energy Phys.* **0205** (2002) 059.
- [17] T.R. Morris, *Nucl. Phys.* **B 495** (1997) 477.
- [18] S. Arnone, A. Gatti and T. R. Morris, *Acta Phys. Slov.* **52** (2002) 621, [hep-th/0209130](#).
- [19] Tim R. Morris and John F. Tighe, *J. High Energy Phys.* **08** (1999) 7.
- [20] T. Papenbrock and C. Wetterich, *Z. Phys. C* **65** (1995) 519, [hep-th/9403164](#).
- [21] M. Bonini, G. Marchesini and M. Simionato, *Nucl. Phys. B* **483** (1997) 475, [hep-th/9604114](#).
- [22] M. Pernici and M. Raciti, *Nucl. Phys. B* **531** (1998) 560, [hep-th/9803212](#).
- [23] P. Kopietz, *Nucl. Phys. B* **595** (2001) 493 [hep-th/0007128](#).
- [24] D. Zappala, *Phys. Rev. D* **66** (2002) 105020, [hep-th/0202167](#).
- [25] S. Arnone, A. Gatti, T.R. Morris and O.J. Rosten, work in progress.
- [26] R.D. Ball, P.E. Haagensen, J.I. Latorre and E. Moreno, *Phys. Lett. B* **347** (1995) 80;
- [27] D. V. Shirkov, *Theor. Math. Phys.* **60** (1985) 778.
- [28] S. Arnone, Yu. Kubyshin, T.R. Morris and J.F. Tighe, *Int. J. Mod. Phys. A* **17**, **Vol. 17** (2002) 2283, [hep-th/0106258](#).
- [29] Thus no further bilinear term must be hiding in  $S^{int}$ , at the classical level.
- [30] If  $\sigma$  has an  $O(\lambda^0)$  coefficient, the only other possibility arises, namely that the physical mass is infinite. This will be dealt with in the next gauge theory paper.
- [31] as usual ignoring in perturbation theory, the triviality problems of scalar field theory
- [32] The term in braces depends only on  $q^2/\Lambda^2$ .  $\Omega_4$  is the four dimensional solid angle. The last line follows from the convergence of the integral and normalization conditions,  $c(0) = 1$  and  $S_0^{(4)}(\vec{0}) = 1$ .
- [33] It should be evaluated at order  $p^2$ , but divergences cancel at any order.
- [34] Remember  $S_1^{(4)}(\vec{0})$  is zero by the renormalization condition, so there is no infrared divergence in iii.
- [35] In this case, divergent even after performing  $\Lambda\partial_\Lambda$ .
- [36] The same symbol is used for the 4-vector and its modulus. It should hopefully be clear from the context what we mean by it.